

# Probing CKM via Semileptonic B Decays at the $\Upsilon(4S)$

K. Kinoshita

*University of Cincinnati*

Semileptonic decays of  $B$  mesons may be used in many different ways to probe the CKM matrix. Presented here are several recent results from the CLEO II experiment, all involving the analysis or utilization of semileptonic  $B$  decays.

## I. INTRODUCTION

One of the major goals for the study of weak decays of the  $B$  meson is the measurement of several third generation elements in the Cabibbo-Kobayashi-Maskawa (CKM) matrix with sufficient accuracy to determine whether the matrix is unitary. The requirement of unitarity constrains the number of free parameters in this matrix to four. The four are often shown in the explicit form

$$\begin{pmatrix} 1 - \frac{\lambda^2}{2} & \lambda & \lambda^3 A(\rho - i\eta) \\ -\lambda & 1 - \frac{\lambda^2}{2} & \lambda^2 A \\ \lambda^3 A(1 - \rho - i\eta) & -\lambda^2 A & 1 \end{pmatrix}.$$

One condition of unitarity is that the scalar product of any column with the complex conjugate of any other equals zero which, when applied to the first and third columns, gives

$$0 = V_{ub}^* V_{ud} + V_{cb}^* V_{cd} + V_{tb}^* V_{td}$$

When divided by the second term

$$0 = \frac{V_{ub}^* V_{ud}}{V_{cb}^* V_{cd}} + 1 + \frac{V_{tb}^* V_{td}}{V_{cb}^* V_{cd}}$$

and presented explicitly in terms of the parameters  $\rho$  and  $\eta$ , this constraint may be illustrated graphically as a triangle in the complex plane, as shown in Figure 1. This triangle is known as a “unitarity triangle.”

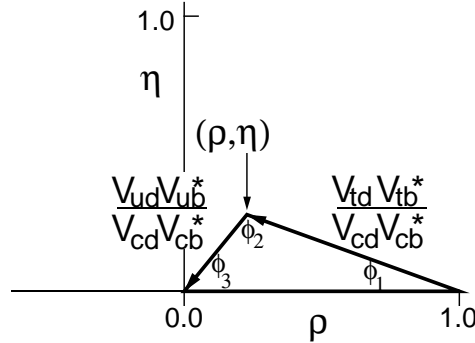


FIG. 1. “Unitarity triangle” in  $\rho - \eta$  complex plane.

The least known of these CKM elements are those involving  $b$  or  $t$ , and by studying the partial rates to selected  $B$  decay modes, one is effectively measuring the lengths of the sides of this triangle. In this talk I report recent results from the CLEO II experiment for  $\bar{B} \rightarrow D\ell^-\bar{\nu}$ ,  $\bar{B} \rightarrow (\pi/\rho/\omega)\ell^-\bar{\nu}$ , and  $B^0$  mixing, which are sensitive to the elements  $|V_{cb}|$ ,  $|V_{ub}|$ , and  $|V_{td}|$  respectively, through the processes illustrated in Figure 2.

## II. DATA

The data were collected with the CLEO II detector [1] at the Cornell Electron Storage Ring (CESR). Most of the results reported here were obtained using a sample of  $e^+e^-$  annihilation events collected during the period 1990-5,

with an integrated luminosity  $3.1 \text{ fb}^{-1}$  on the  $\Upsilon(4S)$  resonance ( $\sqrt{s} = 10.58 \text{ GeV}$ ) and  $1.13 \text{ fb}^{-1}$  at a center-of-mass energy which is lower by 60 MeV (continuum).

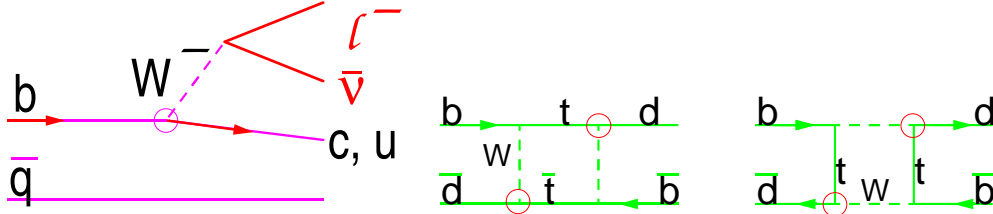


FIG. 2. Processes used to measure CKM elements. (left) Semileptonic decay:  $b \rightarrow c$  probes  $|V_{cb}|$  and  $b \rightarrow u$  is sensitive to  $|V_{ub}|$ . (center, right) Examples of “box” diagrams describing  $B^0$  mixing, sensitive to  $|V_{td}|$ .

The proximity of the  $\Upsilon(4S)$  resonance to the  $B\bar{B}$  mass threshold and the  $B$  meson’s lack of spin make the process  $e^+e^- \rightarrow \Upsilon(4S)$  particularly amenable to the experimental study of  $B$  decays. Because the resonance is only 20 MeV above the  $B\bar{B}$  mass threshold, nearly all resonance events decay exclusively to  $B\bar{B}$ , with roughly equal numbers to charged and neutral mesons. At the same time, each  $B$  is very slow,  $\beta\gamma \approx 0.06$ , so the assumption that the lab frame is the  $B$  center of mass is a useful approximation in many cases. Because the  $B$  is spinless, the angular distributions of decay products from one  $B$  are uncorrelated with those from the other. As a consequence, the event as a whole tends to have a spherical rather than jetty shape, and the decay of each  $B$  may be treated as an event with energy  $\sqrt{s}/2$  in its center of mass.

The low speed of the  $B$  in the lab frame enables the use of a method known as “partial reconstruction,” where an exclusive decay mode is identified through one or more particles that are detected (Y) and one that is not (X). As all of the analyses reported in this talk exploit this method to some degree, I present here a brief outline to which later discussions will refer. The requirements of energy-momentum conservation

$$E_X = E_B - E_Y, \quad \vec{p}_X = \vec{p}_B - \vec{p}_Y$$

which lead explicitly to the mass constraint

$$\begin{aligned} M_X^2 &= E_X^2 - |\vec{p}_X|^2 \\ &= (E_B - E_Y)^2 - |\vec{p}_B|^2 - |\vec{p}_Y|^2 + 2|\vec{p}_B||\vec{p}_Y|\cos\theta_{B,Y} \end{aligned} \quad (1)$$

form the basis for this method. In the equation (1) only the quantity  $\cos\theta_{B,Y}$  is unknown. In one approach, the lab frame is taken to be the center of mass ( $|\vec{p}_B| = 0$ ) so that the “missing mass squared” is approximated as

$$M_X^2 \approx (E_B - E_Y)^2 - |\vec{p}_Y|^2. \quad (2)$$

Its distribution peaks broadly around the expected value. In another approach, one examines the distribution of  $\cos\theta_{B,Y}$ :

$$\cos\theta_{B,Y} = \frac{M_B^2 + M_Y^2 - M_X^2 - 2E_BE_Y}{2|\vec{p}_B||\vec{p}_Y|} \quad (3)$$

where one can expect correctly reconstructed candidates to give physical values,  $|\cos\theta_{B,Y}| < 1$ .

### III. $|V_{CB}|$ VIA $\bar{B} \rightarrow D\ell^-\bar{\nu}$

From a theoretical point of view, the relationship of  $|V_{cb}|$  to the partial width  $\Gamma(\bar{B} \rightarrow D\ell^-\bar{\nu})$  is the product of the relevant couplings, kinematic terms, and a hadronic form factor  $F_D$ , which is a function of  $w \equiv \frac{m_B^2 + m_D^2 - q^2}{2m_B m_D}$  ( $1.00 < w < 1.59$ ):

$$\frac{d\Gamma}{dw} = \frac{G_F^2 |V_{cb}|^2}{48\pi^3} (m_B + m_D)^2 m_D^3 (w^2 - 1)^{3/2} F_D(w)^2$$

$F_D$  is usually expressed in a form with one or two free parameters, for example the quadratic form

$$\frac{F_D(w)}{F_D(1)} \approx 1 - \rho_D^2 (w - 1) + c_D (w - 1)^2 \quad (4)$$

Experimentally, the measured estimator  $\tilde{w}$  is only a fair approximation to  $w$  because the neutrino is not well measured, so the shape of the original (root) distribution is distorted. To regain the root distribution we measure the rate  $\delta\tilde{\Gamma}_i(\tilde{w})$  in ten bins and unfold via an efficiency matrix  $\epsilon_{ij}$ :  $\delta\Gamma_i = \epsilon_{ij}^{-1} \delta\tilde{\Gamma}_j$ . The unfolded distribution is then fitted for  $|V_{cb}|$  and the shape of  $F_D$ , using several parametrized forms of  $F_D$ .

At the  $\Upsilon(4S)$ , the decay is reconstructed inclusively to obtain the product branching fractions

$$\begin{aligned} \mathcal{B}(\Upsilon(4S) \rightarrow B^0 \bar{B}^0) \frac{d\mathcal{B}}{d\tilde{w}} (\bar{B}^0 \rightarrow D^+ \ell^- \bar{\nu}) &\equiv f_{00} \frac{dB_0}{d\tilde{w}} \\ \mathcal{B}(\Upsilon(4S) \rightarrow B^+ B^-) \frac{d\mathcal{B}}{d\tilde{w}} (B^- \rightarrow D^0 \ell^- \bar{\nu}) &\equiv f_{+-} \frac{dB_-}{d\tilde{w}} \end{aligned}$$

where  $f_{00}(f_{+-})$  is the fraction of charged (neutral) events, and  $f_{00} + f_{+-} = 1$ . These are unfolded to get root differential branching fractions, which are then related to the differential width by

$$\begin{aligned} \frac{d\Gamma}{dw} &= \frac{1}{\tau_-} \frac{dB_-}{dw} = \frac{1}{\tau_0} \frac{dB_0}{dw} \\ &= \frac{1}{\tau_-} \left( f_{+-} \frac{dB_-}{dw} \right) + \frac{1}{\tau_0} \left( f_{00} \frac{dB_0}{dw} \right) \end{aligned}$$

Measured in this way,  $d\Gamma/dw$  is independent of  $f_{00}$ , which is not well measured.

Using  $3.1 \text{ fb}^{-1}$  of CLEO data, candidates consist of an identified electron or muon and a candidate for  $D^0 \rightarrow K^- \pi^+$  or  $D^+ \rightarrow K^- \pi^+ \pi^+$ . For each mode the distribution in the quantity  $\cos\theta_{B,D\ell}$  (described by equation (3)) is examined. Backgrounds include candidates containing a fake  $D$  or lepton,  $D$  and  $\ell$  from opposite  $B$ 's, continuum events, and  $D - \ell$  combinations from  $B$  decay modes such as  $B \rightarrow DX\tau\nu$  ( $\tau \rightarrow \ell X$ ) or  $B \rightarrow D_s D$  ( $D_s \rightarrow \ell X$ ). For each mode the distribution remaining after these background subtractions is shown in Figure 3 and includes, in addition to the signal mode, large contributions from modes  $B \rightarrow DX\ell\nu$  where  $DX$  originate with  $D^*$ ,  $D^{**}$ , or nonresonant  $D^{(*)}\pi$  states. To extract the distribution in  $\tilde{w}$  of  $B \rightarrow D\ell\nu$ , the  $\cos\theta_{B,D\ell}$  distribution is fitted to a sum of simulated shapes for these modes, in each of the ten bins of  $\tilde{w}$  (Figure 4). This distribution is then unfolded to obtain the root distribution, which is fitted to several theoretical forms [2].

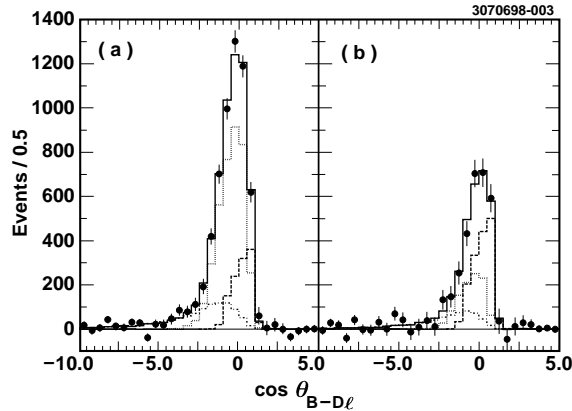


FIG. 3. Distributions in  $\cos\theta_{B,D\ell}$  for (a)  $B \rightarrow D^0 X \ell \nu$  and (b)  $B \rightarrow D^+ X \ell \nu$ , data (solid circles) with results from fitting to simulations (solid histogram), which include contributions from  $B \rightarrow D \ell \nu$  (dashed),  $B \rightarrow D^* \ell \nu$  (dotted), and  $B \rightarrow D^{**} \ell \nu + D^{(*)} \pi \ell \nu$  (dash-dotted).

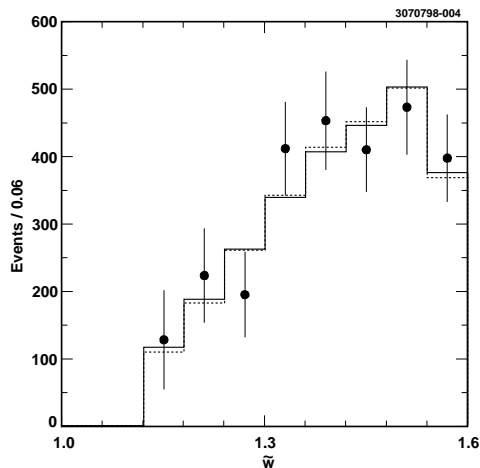


FIG. 4. The sum of  $B^- \rightarrow D^0 \ell^- \bar{\nu}$  and  $\bar{B}^0 \rightarrow D^+ \ell^- \bar{\nu}$  yields as a function of  $\tilde{w}$ , for the data (solid circles) and from the best fit linear form factor (dashed histogram) or dispersion relation inspired form factor of Boyd *et al.* (solid histogram).

The results for partial width and branching fractions are

$$\begin{aligned}\Gamma(B \rightarrow D \ell \nu) &= (14.1 \pm 1.0 \pm 1.2) \text{ns}^{-1} \\ \mathcal{B}(B^- \rightarrow D^0 \ell^- \bar{\nu}) &= (2.32 \pm 0.17 \pm 0.20)\% \\ \mathcal{B}(B^0 \rightarrow D^+ \ell^- \bar{\nu}) &= (2.20 \pm 0.16 \pm 0.19)\%\end{aligned}$$

These are combined with a previous CLEO result [3] to obtain

$$\begin{aligned}\Gamma(B \rightarrow D \ell \nu) &= (13.4 \pm 0.8 \pm 1.2) \text{ns}^{-1} \\ \mathcal{B}(B^- \rightarrow D^0 \ell^- \bar{\nu}) &= (2.21 \pm 0.13 \pm 0.19)\% \\ \mathcal{B}(B^0 \rightarrow D^+ \ell^- \bar{\nu}) &= (2.09 \pm 0.13 \pm 0.18)\%\end{aligned}$$

Using  $F_D(1) = 1.0$  gives

$$|V_{cb}| = 0.045 \pm 0.006 \pm 0.004 \pm 0.005$$

where the errors are statistical, systematic, and theoretical, due to uncertainty in  $F_D(1)$ . This result is consistent with the most precise current value,  $|V_{cb}| = 0.0395 \pm 0.0017$  [4], obtained using the decay  $B \rightarrow D^* \ell \nu$ .

#### IV. $|V_{UB}|$ VIA EXCLUSIVE SEMILEPTONIC DECAYS

At present, semileptonic  $B$  decays are the only ones which are able to provide measurements of  $|V_{ub}|$ . Experimentally, the measurement is difficult because the rate is small and the decays can be studied only in limited kinematic regions where they are not overwhelmed by backgrounds from the much more abundant  $b \rightarrow c$  decays. The difficulty is compounded by the spread among theoretical models which provide the relationship between measured rates and the matrix element. In this context, exclusive and inclusive semileptonic decays yield measurements of  $|V_{ub}|$  in somewhat complementary ways. Presented here is a measurement using five exclusive modes and a method that differs from that used in the previously published CLEO II result based on the same modes [5].

To identify an exclusive decay, a track is identified as an electron or muon and combined with a  $u$ -hadron candidate ( $\rho^\pm \rightarrow \pi^\pm \pi^0$ ,  $\rho^0 \rightarrow \pi^+ \pi^-$ ,  $\omega \rightarrow \pi^+ \pi^- \pi^0$ ,  $\pi^0 \rightarrow \gamma \gamma$ , or  $\pi^\pm$ ). In addition, a neutrino candidate is formed based on missing momentum and energy in the event. The three-particle combination must be kinematically consistent with originating from a  $B$  decay. The principal background in the most significant kinematic regions arises from continuum events, so requirements are designed to suppress these strongly. The following constraints, which are due to light quark symmetry, are applied:

$$\begin{aligned}
\Gamma(\bar{B}^0 \rightarrow \rho^+ \ell^- \bar{\nu}) &= 2\Gamma(B^- \rightarrow \rho^0 \ell^- \bar{\nu}) \\
&= 2\Gamma(B^- \rightarrow \omega^0 \ell^- \bar{\nu}) \\
\Gamma(\bar{B}^0 \rightarrow \pi^+ \ell^- \bar{\nu}) &= 2\Gamma(B^- \rightarrow \pi^0 \ell^- \bar{\nu})
\end{aligned}$$

The candidates are sorted by lepton momentum into three samples, [2.3-2.7], [2.0-2.3], and [1.7-2.0] GeV/c. A maximum likelihood fit is then performed for all three samples on distributions of the five modes in the quantity  $\Delta E$ , defined as the candidate energy minus the beam energy and, where applicable, the invariant mass of the  $\rho$  or  $\omega$  candidate. The fit accounts for contributions not only from the signal modes but also from other decays of the type  $b \rightarrow u\ell\nu$ ,  $b \rightarrow c$  semileptonic decays, fake leptons, and continuum. To allow for uncertainties in the contribution from  $b \rightarrow c$  modes, each bin of lepton momentum is normalized separately, although the normalization among distributions within each bin is common. A total of twelve free parameters remain in the fit. A projection onto the  $\pi\pi$  invariant mass of the fit for the sum of  $\rho$  modes in the highest lepton momentum bin is shown in Figure 5. We obtain a result for the branching fraction  $\mathcal{B}(\bar{B}^0 \rightarrow \rho^+ \ell^- \bar{\nu})$  assuming that neutral and charged  $B$ 's are produced in equal abundance at the  $\Upsilon(4S)$ . From the branching fraction and the measured  $B^0$  lifetime [4] we obtain the partial width and  $|V_{ub}|$ .

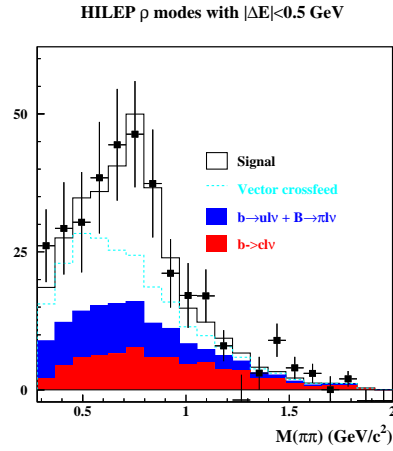


FIG. 5. Projection of maximum likelihood fit onto  $\pi\pi$  invariant mass in the highest lepton momentum bin for the sum of  $\rho$  modes. For this plot a requirement of  $|\Delta E| < 500$  MeV has been made.

Both the reconstruction efficiency and extraction of  $|V_{ub}|$  from the measurement are somewhat model-dependent. To estimate the degree of uncertainty due to models, the analysis is repeated for each of five current models [6]. The resulting values are presented in Figure 6. For each result the average is given as the central value and the model dependence error is taken to be half the full spread among the five results. This measurement of  $|V_{ub}|$  is comparable to that obtained via inclusive semileptonic decays,  $|V_{ub}| = (3.2 \pm 0.8) \times 10^{-3}$  [4]. These results are largely independent of our previously published result [5]. An average which takes into account the statistical and systematic correlations will be presented in the near future.

It may be possible to address the uncertainties due to model dependence through the measurement of the decay rate as a function of  $q^2$ . To investigate this possibility, the data were subdivided into three bins, [0-7], [7-14], and [14-21]  $(\text{GeV}/c^2)^2$ , the maximum allowed by current statistics. The results for the partial widths  $\Delta\Gamma(B \rightarrow \rho\ell\nu)$  are

$$\begin{aligned}
(7.6 \pm 3.1_{-1.2}^{+0.9} \pm 3.1) \times 10^{-5} \text{ps}^{-1} & \quad 0 < q^2 < 7 \text{ GeV}^2/c^4 \\
(4.8 \pm 2.9_{-0.8}^{+0.7} \pm 0.7) \times 10^{-5} \text{ps}^{-1} & \quad 7 < q^2 < 14 \text{ GeV}^2/c^4 \\
(7.1 \pm 2.1_{-1.1}^{+0.9} \pm 0.6) \times 10^{-5} \text{ps}^{-1} & \quad 14 < q^2 < 21 \text{ GeV}^2/c^4
\end{aligned}$$

where the errors are statistical, systematic, and model spread, respectively. The highest of these bins has the smallest model variation.

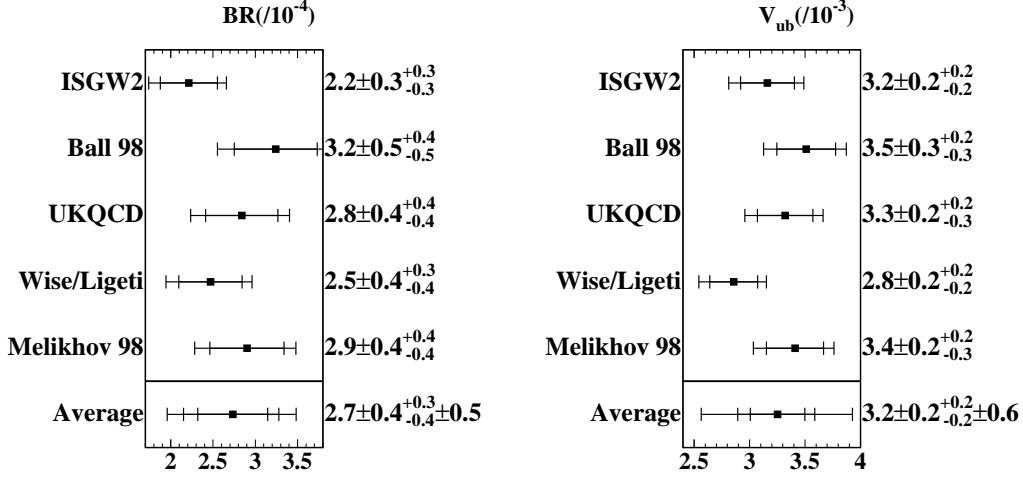


FIG. 6. Branching fraction  $\mathcal{B}(\bar{B}^0 \rightarrow \rho^+ \ell^- \bar{\nu})$  (left) and  $|V_{ub}|$  (right) for five models, with averages (preliminary).

### V. $|V_{TD}|$ VIA $B^0$ MIXING

Mixing occurs for neutral  $B$  mesons through second order weak processes such as those represented in the box diagrams in Figure 2. It causes the exponential decay pattern of a population of  $B$ 's to contain an oscillatory component, as is illustrated for a hypothetical case in Figure 7. The oscillation rate  $\omega$  is proportional to  $|V_{td}|^2$ , and the fraction  $\chi_d$  of an initial population of  $B^0$  that eventually decays as  $\bar{B}^0$  may be expressed in terms of the product  $\omega\tau \equiv x_d$  where  $\tau$  is the lifetime:

$$1 - \chi_d = \frac{2 + x_d^2}{2(1 + x_d^2)}$$

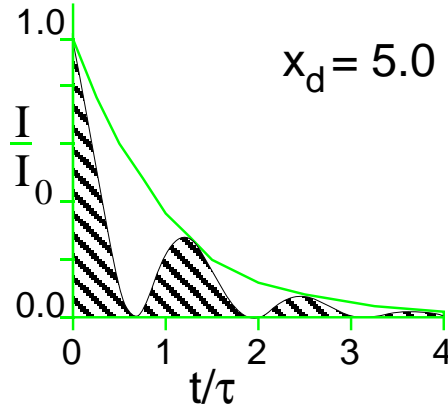


FIG. 7. Illustration of mixing:  $B$  decays observed given an initial population of pure  $B$ , for  $x_d = 5.0$

At the  $\Upsilon(4S)$ , mixing is manifested by the presence of “mixed” events, where two  $B$  decays of the same flavor,  $B^0 B^0$  or  $\bar{B}^0 \bar{B}^0$ , are found in the same event. In this case,  $\chi_d$  is equal to the fraction of mixed events among neutral  $B$  events.

Presented here are two methods of tagging that enable the clean flavor identification of both  $B$ 's in an event. In tagging, the objective is to reconstruct one of the  $B$ 's sufficiently to identify its flavor and to identify it as a neutral  $B$ . The flavor of the second  $B$  is then identified through a lepton with high momentum, which originates predominantly from decays of the type  $B \rightarrow c \ell \nu$ . The tagging is accomplished through partial reconstruction of two different decay modes:

1.  $\bar{B}^0 \rightarrow D^{*+}\ell^-\bar{\nu}$   $\{D^{*+} \rightarrow D^0\pi_s^+\}$ , where two of the particles,  $\bar{\nu}$ ,  $D^0$  are not detected but can be constrained due to the kinematics of  $B$  and  $D^*$  decays:

$$E_{D^*} \approx E_{\pi_s} \frac{M_{D^*}}{E_{\pi}^{CM}} \equiv \tilde{E}_{D^*} \quad \tilde{p}_{D^*} \equiv \hat{p}_{\pi_s} \sqrt{\tilde{E}_{D^*}^2 - m_{D^*}^2}$$

$$\Rightarrow \widetilde{M}_\nu^2 = (E_B - E_\ell - \tilde{E}_{D^*})^2 - |\vec{p}_B - \vec{p}_\ell - \tilde{p}_{D^*}|^2$$

2.  $\bar{B}^0 \rightarrow D^{*+}(\pi^-/\rho^-)$   $\{D^{*+} \rightarrow D^0\pi_s^+\}$ , where the  $D^0$  is not detected but can be fully constrained (except for a twofold ambiguity) through energy and momentum conservation.

To identify  $\bar{B}^0 \rightarrow D^{*+}\ell^-\bar{\nu}$ , we select a high momentum ( $> 1.4$  GeV/c) electron or muon and a soft track ( $< 0.190$  GeV/c) with the opposite charge. For signal candidates, where the pair originate from the signal decay as specified above, the distribution in  $\widetilde{M}_\nu^2$  form a peak centered near  $\widetilde{M}_\nu^2 = 0$ , as shown in Figure 8. The backgrounds are formed from random combinations of leptons and soft tracks and may originate in continuum or  $\Upsilon(4S)$  events. Continuum backgrounds may be estimated using our nonresonant data sample, and backgrounds from  $B\bar{B}$  events are estimated via Monte Carlo simulation.

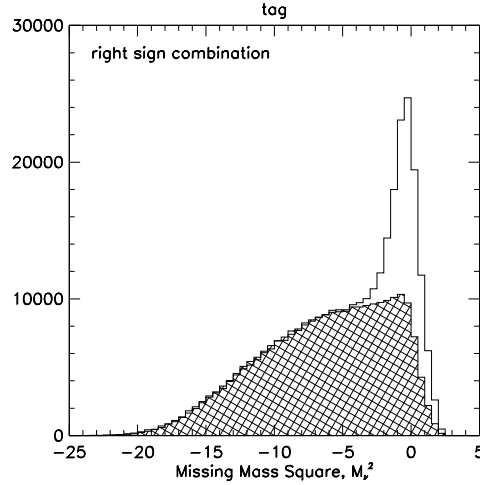


FIG. 8. Distributions in  $\widetilde{M}_\nu^2 = 0$  of candidates for  $\bar{B}^0 \rightarrow D^{*+}\ell^-\bar{\nu}$ , data with continuum contribution subtracted (solid) and simulated background (cross-hatched).

Candidates are further sorted according to the momentum of any additional leptons that are identified in the event and whether the additional lepton has the opposite (“unmixed”) or same (“mixed”) charge as the lepton of the tag. For each sorted set, the number of tags is extracted according to the same procedure. The additional leptons are mainly from primary decays of the type  $b \rightarrow c(u)\ell^-\bar{\nu}$  and secondary decays  $b \rightarrow cX\{c \rightarrow s\ell^+\nu\}$ . Leptons from other sources, including hadrons misidentified as leptons, secondary leptons from decays of  $B$  to  $\psi$ ,  $\Lambda_c$ ,  $\tau$ , and  $\bar{c}$ , and electrons from  $\gamma \rightarrow e^+e^-$  and  $\pi^0 \rightarrow \gamma e^+e^-$  are accounted for and subtracted. The net number in each bin is corrected for the detection efficiency of the additional lepton.

The resulting lepton momentum distributions are shown in Figure 9. Each is fitted to a sum of primary and secondary spectrum shapes to extract the net number of primary leptons with mixed or unmixed events. The mixing parameter  $\chi_d$  is straightforwardly derived from the ratio of the two fitted numbers.

To reconstruct  $\bar{B}^0 \rightarrow D^{*+}(\pi^-/\rho^-)$ ,  $\{D^{*+} \rightarrow D^0\pi_s^+\}$ , we select candidates consisting of a hard track or  $\rho^\pm$  candidate ( $p_h > 1.4$  GeV/c) and a soft track with opposite charge. These are required to be kinematically consistent with being the hard hadron and the soft pion from  $D^*$  originating with the signal decay, and this constraint is sufficient to yield a high signal relative to background. Events containing tag candidates are then searched for a hard lepton ( $p_l > 1.4$  GeV/c) and sorted as an “unmixed” event if the hard hadron and lepton have opposite charge and as a

“mixed” event if they have the same charge. The mixing parameter  $\chi_d$  is extracted by accounting for the various correlated contributions to the mixed and unmixed samples, including true mixing, continuum, and background candidates from  $B^0$  and from  $B^-$ .

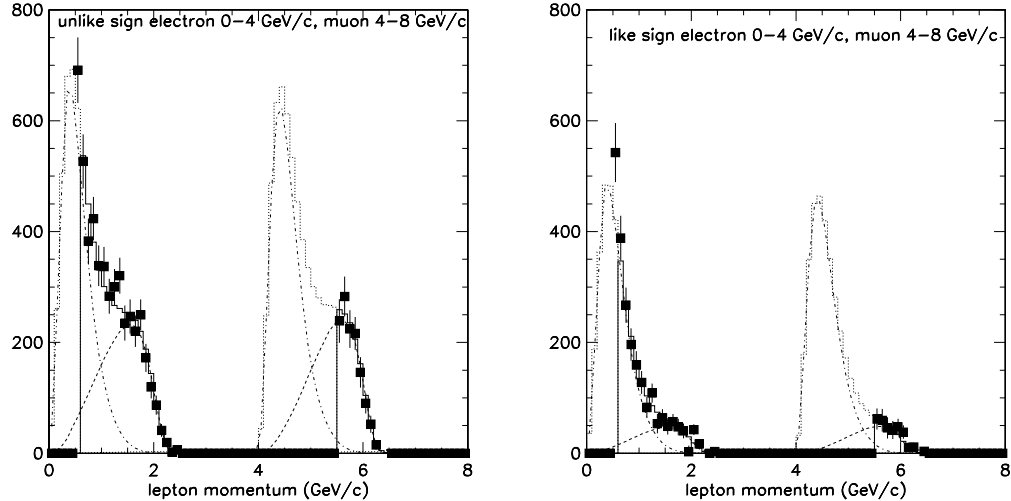


FIG. 9. Distributions of additional leptons in events containing  $\bar{B} \rightarrow D^{*+} X \ell \bar{\nu}$ , shown with fits to primary (dashed) and secondary (dash-dotted) spectra. Electron momentum is plotted in the region 0.0-4.0 GeV/c and {muon momentum+4.0 GeV} is plotted in the region 4.0-8.0 GeV/c. In the left plot the two leptons have opposite charge (unmixed), and in the right plot they have the same charge (mixed).

Preliminary results for both of these mixing analyses are presented here. Using the tag of  $\bar{B} \rightarrow D^{*+} \ell \bar{\nu}$  with  $3.1 \text{ fb}^{-1}$  of data we find

$$\begin{aligned}\chi_d &= 0.187 \pm 0.019 \pm 0.007 \\ x_d &= 0.773 \pm 0.048 \pm 0.018 \\ |V_{td}| &= 0.0086 \pm 0.0003 \pm 0.0001 \pm 0.0018\end{aligned}$$

where the third error on  $|V_{td}|$  is due to uncertainties in the theory. The result from the  $\bar{B}^0 \rightarrow D^{*+} (\pi^- / \rho^-)$  tag with  $3.99 \text{ fb}^{-1}$  of data is

$$\chi_d = 0.191 \pm 0.026 \pm 0.014$$

Both analyses are comparable in statistical significance to the best previous results but have significantly reduced systematic errors and should result in improvements with larger data sets. However, the determination of  $|V_{td}|$  is currently limited by theoretical uncertainties, which will need to be reduced before these result in better values.

## VI. SUMMARY

Semileptonic  $B$  decays are important for the study of the third generation CKM matrix elements and for investigating the unitarity of the matrix. Recent measurements of the rates for  $B \rightarrow D \ell \nu$ ,  $B \rightarrow (\rho/\omega/\pi) \ell \nu$ , and  $B^0$  mixing by the CLEO II experiment have been presented here. These rates are sensitive to  $|V_{cb}|$ ,  $|V_{ub}|$ , and  $|V_{td}|$ , respectively. These measurements highlight the progress being made in the development of experimental techniques and in the theoretical understanding of the dynamics of heavy quark decay.



- [1] Y. Kubota *et al.*, *Nucl. Instrum. Methods* **A320**, 66 (1992).
- [2] C. G. Boyd, B. Grinstein, and R.F. Lebed, *Phys. Rev.* **D56**, 6895 (1997); I. Caprini, L. Lellouch, and M. Neubert, *Nucl. Phys.* **B530**, 153 (1998); Form of equation (4), with and without quadratic term.
- [3] M. Athanas *et al.*, *Phys. Rev. Lett.* **79**, 2208 (1997).
- [4] “Review of Particle Physics,” *Eur. Phys. J.* **C3**, 1 (1998).
- [5] J. Alexander *et al.*, *Phys. Rev. Lett.* **77**, 5000 (1996).
- [6] N. Isgur and D. Scora, *PR* **D52**, 2783 (1995); L. Del Debbio *et al.*, *Phys. Lett.* **B416**, 393 (1998); P. Ball and V.M. Braun, *PR* **D58**, 094016 (1998); M. Beyer and D. Melikhov, *PL* **B436**, 344 (1998); Z. Ligeti and M. B. Wise, *PR* **D53**, 4937 (1996).